Gene Expression, Vol. 12, pp. 177–192
Printed in the USA.

1052-2166/05 $20.00 + .00
E-ISSN 1555-3884
www.cognizantcommunication.com

Transcriptional Modulations by RXR Agonists Are Only Partially Subordinated to PPARα Signaling and Attest Additional, Organ-Specific, Molecular Cross-Talks

PASCAL G. P. MARTIN,* FRÉDÉRIC LASSERRE,* CÉCILE CALLEJA,*[1] ARMELLE VAN ES,*[1] ALAIN ROULET,* DIDIER CONCORDET,† MICHELA CANTIELLO,‡ ROMAIN BARNOUIN,*[1] BÉATRICE GAUTHIER,§ AND THIERRY PINEAU*

**Laboratoire de Pharmacologie et Toxicologie, I.N.R.A., BP3, Toulouse, France*
†UMR 181, I.N.R.A./E.N.V.T., Toulouse, France
‡Dipartimento di Patologia Animale, Universita'degli Studi di Torino, Torino, Italy
§Galderma R&D, Sophia-Antipolis, France

Nuclear hormone receptors (NR) are important transcriptional regulators of numerous genes involved in diverse pathophysiological and therapeutic functions. Following ligand activation, class II NR share the ability to heterodimerize with the retinoid X receptor (RXR). It is established that RXR activators, rexinoids, transactivate several peroxisome proliferator-activated receptor α (PPARα) target genes in a PPARα-dependent manner. We hypothesized that, once activated, RXR might signal through quiescent NR other than PPARα, in an organ-specific manner. To study this putative phenomenon in vivo, we developed an array of 120 genes relevant to the class II NR field. The genes were selected using both published data and high-density screenings performed on RXR or PPARα agonist-treated mice. Wild-type C57BL/6J and PPARα-deficient mice were treated with fenofibrate (PPARα activator) or LGD1069 (RXR activator). Using our customized array, we studied the hepatic, cardiac, and renal expression of this panel of 120 genes and compared them in both murine genotypes. The results obtained from this study confirmed the ability of an RXR agonist to modulate PPARα-restricted target genes in the liver and the kidney. Furthermore, we show that various organ-specific regulations occurring in both genotypes (PPARα +/+ or −/−) are highly indicative of the ability of RXR to recruit other class II NR pathways. Further development of this molecular tool may lead to a better understanding of the permissiveness of class II nuclear receptor dimers in vivo.

Key words: Nuclear receptor; RXR; PPAR; Retinoid; Rexinoid; Fibrate; Microarray; PPARα −/−; Cutaneous T-cell lymphoma; Vitamin D

NUCLEAR receptors (NR) are potent transcriptional modulators involved in numerous physiological functions such as embryonic development, cell differentiation, and energy homeostasis. They act as hormones, nutrients, drugs, or pollutants sensors. Upon activation by selective chemicals, NR of the class II transduce their molecular signal by heterodimerizing with the retinoid X receptor (RXRα, β, and γ isoforms/NR2B). In this molecular network, RXR isoforms hold the remarkably central position of a common partner dimerizing with all class members [thyroid hormone receptor (TR/NR1A), retinoic acid receptor

[1]Present address: IGBMC, Illkirch, France.
Address correspondence to Thierry Pineau, Laboratoire de Pharmacologie et Toxicologie, Institut National de la Recherche Agronomique, 180 Chemin de Tournefeuille, BP3, F 31931 Toulouse, Cedex 9, France. Tel: (33) 561 28 53 95; Fax: (33) 561 28 53 10; E-mail: tpineau@toulouse.inra.fr

(RAR/NR1B), peroxisome proliferator-activated receptor (PPAR/NR1C), liver X receptor (LXR/NR1H2 and NR1H3), farnesoid X receptor (FXR/NR1H4 and NR1H5), vitamin D receptor (VDR/NR1I1), pregnane X receptor (PXR/NR1I2), constitutive androstane receptor (CAR/NR1I3 and NR1I4), etc.].

Several molecular signaling pathways elicited from these receptors are drug targets for therapeutic intervention in humans. Fibrates activate PPARα and are potent hypolipidemic drugs. Retinoids that activate more or less specifically the RAR and RXR isoforms are beneficially prescribed for dermatological disorders (acne, psoriasis, photodamage, and cancer). Nevertheless, side effects elicited by retinoids (e.g., teratogenicity, hypertriglyceridemia, mucocutaneous toxicity) led to the development of more selective RXR activators termed rexinoids (6,24). Recently, the FDA approved bexarotene and Targretin (LGD1069; Ligand Pharmaceuticals, San Diego, CA) for the treatment of cutaneous T-cell lymphoma (CTCL). Rexinoids such as LGD1069 and the more potent RXR-selective agonist LG100268 (7) sustain beneficial actions for the treatment of cancers (12,13) and promise well for the treatment of type II diabetes (33) and atherosclerosis (10).

The high selectivity of these molecules towards RXR provides novel chemical probes for molecular investigations. Indeed, it could be envisaged that, following its selective activation, RXR could recruit one or several of its quiescent partners, even in the absence of their own xenobiotic activators, to trigger an original and potentially beneficial pharmacological response. Numerous RXR heterodimers have been initially classified as either permissive or nonpermissive based on their ability to respond to RXR ligands (28). RXR is thought to be ligand inducible in its association with PPAR (17,33), LXR (43), FXR (15), NGFI-B and Nurr1 (14,37). It has been considered a silent partner in its association with TR, VDR, and RAR. However, these assumptions are still a matter of debate and the necessary caution in the definition of dimer permissiveness has been highlighted in a recent study of the RXR-CARβ heterodimer (41). Considering the multiplicity of the factors affecting the activity of each RXR heterodimer (promoter context, endogenous ligands, interactions with other RXR dimerization partners, cofactors expression, phosphorylations), we can expect that the responses would vary depending on the cellular context. We recently exemplified this concept by showing that rexinoid-induced upregulation of mouse pyruvate dehydrogenase kinase 4 is strictly PPARα dependent in the liver and the kidney but PPARα independent in the heart (35).

Considering the theoretical multiple impacts of rexinoids, assessing their net molecular effects would obviously require an integrative biology strategy aimed at recording their organ-specific transcriptional signatures. We thought to develop a customized low-density murine cDNA macroarray dedicated to class II NR pathways to gain information relevance and processing efficiency. This molecular tool allowed us to simultaneously record the level of expression of 120 transcripts, in three organs, under conditions of chemical exposure of the mice.

We thus screened wild-type and PPARα –/– mice treated with LGD1069 (RXR ligand) or fenofibrate (PPARα ligand) for the expression level of these 120 transcripts in liver, kidney, and heart. Fenofibrate and PPARα –/– mice were used because rexinoids are known to induce the PPARα signaling pathway in the liver (32,35). Our results demonstrate a clear activation by LGD1069 of the PPARα signaling pathway in the liver and the kidney but not in the heart. We further identify new organ-specific targets of LGD1069 treatment. These noticeably include lipogenesis-related genes as well as Cyp2b10, Cyp2c29, and Cyp26 in the liver. In the kidney LGD1069 treatment results in induction of two genes implicated in vitamin D_3 homeostasis independently of PPARα expression while the apolipoprotein E transcript is induced solely in the absence of PPARα. These regulations are discussed in light of the actual knowledge about RXR heterodimer permissiveness and the use of rexinoids in cancer therapies.

MATERIALS AND METHODS

Chemicals

RXR selective agonists, LGD1069 and LG100268, were synthesized and controlled by the Chemistry Department at Galderma R&D. LGD1069 and LG100268 are highly selective RXR agonists with equilibrium dissociation constant (K_d) of 14 and 3 nM for RXRα, respectively, and poor agonists for all three RAR isoforms (both molecules have $K_d > 1$ μM) (6,7). Fenofibrate was purchased from Sigma-Aldrich (Saint Quentin Fallavier, France). Suspensions of test compounds were prepared in a 0.5% (w/v) carboxymethyl-cellulose solution in purified water. Biochemical assays were purchased from Sigma-Aldrich.

Animals

PPARα-deficient male mice on a C57BL/6J genetic background (11,23) were bred at INRA transgenic rodent facility according to European Union guidelines for animal care. Age-matched male C57BL/

6J mice were obtained from Charles River France (Les Oncins, France). In vivo studies were conducted under the E.U. guidelines for the use and care of laboratory animals and all protocols were reviewed and approved by the Ethical Committee for Experimentation on Animals from the "Région Midi Pyrénées" (agreement #MP/03/26/07/03).

Experimental Protocol

Oral administrations were performed by gavage once daily (0900 h) for 8 consecutive days. Mice were fasted 2 h prior to euthanasia by cervical dislocation. The selected organs were dissected, weighed, snap-frozen in liquid nitrogen, and stored at −80°C until RNA extraction.

Triglycerides and Apolipoproteins Measurements

Serum triglycerides, apoA-I and apoB measurements were performed as previously detailed (35).

RNA Isolation

Total RNA was extracted with TRIzol® reagent (Invitrogen, Cergy Pontoise, France) according to the manufacturer's instructions.

Northern Blot Analysis

The procedures used for RNA electrophoretic separation, capillary transfer onto nylon membranes, and hybridization with ^{32}P-radiolabeled cDNA probes were previously detailed (35).

Gene Expression Microarray Analysis Using Incyte® Mouse Unigene 1 Templates

Frozen total RNA samples (200 µg) were provided to Incyte Genomics, Inc. (Palo Alto, CA, USA) for polyA messenger purification. Two samples (LG100268-treated mice and vehicle-treated mice) were analyzed. Taking into account the potential interindividual variability of the response to the drug, each sample consisted of a mix of equal amounts of RNAs extracted from three animals. The quality of the final samples was assessed by electrophoresis on an ethidium bromide-containing agarose gel, prior to shipment. Cy3 and Cy5 fluorescent labeling of the cDNAs was performed while the corresponding messengers were reverse transcribed. Both samples were competitively hybridized on a Mouse Unigene 1 glass template containing 9596 elements from the IMAGE Consortium library. Final data were delivered as a HTML file. Gene names were assigned based on Unigene (build #136) clusters, which include the corresponding IMAGE clone.

Class II NR-Dedicated Macroarray: INRARRAY 01.2

We selected a set of 120 relevant genes (rationale presented in the Results section) to design our original dedicated array. A fragment of each of these genes was amplified by PCR using murine cDNA and selective primer pairs. Each individual fragment was cloned into the pCR®2.1 TOPO® vector (Invitrogen) according to the manufacturer's protocols, thus allowing future cDNAs amplifications using "universal" vector-based primers located on both edges of the cloning site. All plasmids were produced using QIAfilter plasmid maxikit (Qiagen, Courtaboeuf, France). All cloned cDNA were subjected to control analyses (minimum of three restriction fragments analysis and full-length sequencing, especially in the case of failure to integrally produce all expected restriction patterns; 46 clones fully sequenced). A comprehensive list of 120 gene names, corresponding acronyms, GenBank accession numbers, PCR primer sequences, PCR conditions, and probe length can be obtained as supplemental material (http://www.inra.fr/Internet/Centres/toulouse/pharmacologie/pharmacomoleculaire/valorisations/materiel.html). In addition to our own controls (housekeeping genes 36B4 and β-actin, sunflower rubisco-protein large subunit), negative, calibration, and ratio controls used in these experiments were provided by the Lucidea Universal Scorecard (23 artificial genes designed from yeast intergenic regions; Amersham Biosciences, Orsay, France).

Finally, individual cDNA solutions [200 ng µl^{-1}, 50% (v/v) in DMSO] were prepared and spotted as duplicates onto 19 cm^2 positively charged nylon membranes (Immobilon™-Ny+, Millipore, Guyancourt, France) at the Genopole facility in Toulouse, France (http://genopole.toulouse.inra.fr/) with a customized Eurogridder microarrayer (Virtek/Biorad, Marnes-la-Coquette, France).

Quality and concentration of TRIzol®-extracted RNAs were assessed using a 2100 Bioanalyzer (Agilent Technologies, Massy, France). Labeling by random primed reverse transcription was performed on 2 µg of total RNA using the Hotscribe™ kit (Amersham Biosciences, Orsay, France) with 40 µCi of [α-^{33}P]dCTP (MP Biomedicals, Orsay, France). RNA matrix was degraded by alkaline lysis (SDS 0.2%, EDTA 50 mM, and NaOH 300 mM final, 68°C, 45 min). Following neutralization (Tris-HCl, pH 7.5, 500 mM final), unincorporated nucleotides were re-

moved on Sephadex G50 columns (ProbeQuant™ G-50 Micro columns, Amersham Biosciences). The activity of an aliquot was measured (Beta V β-counter, Kontron Instruments, Watford, UK) and the remaining probe was heated (95°C, 5 min) before being added to the hybridization solution (6×10^6 cpm ml^{-1}). Membranes were prehybridized (65°C, 6 h) and hybridized (65°C, 24 h) in a rotating oven (QBiogene, Illkirch, France) in 60-ml individual polypropylene tubes (Nalge Nunc, Rochester, NY, USA) containing 5 ml of hybridization solution (5 × SSC, 5 × Denhardt's solution, 0.5% SDS, 100 μg ml^{-1} salmon sperm DNA). Following washing steps (65°C, 30 min twice and 65°C, 1 h once in 10 ml of 0.1 × SSC, 0.1% SDS) the membranes were exposed for 48–72 h to a phosphor screen before being scanned (50 μm resolution) using a Storm phosphorimager (Amersham Biosciences). Image analysis was performed with ImageMaster™ Array software v2.0 (Amersham Biosciences) with a background correction calculated on the median of spots edge.

Statistical Analysis of INRARRAY *01.2 Data*

All data analyses were performed using the SPlus® 2000 software (Insightful, Toulouse, France) and Multidim library (http://www.lsp.ups-tlse.fr/Carlier/Logiciel.html) for multidimensional statistical analyses. The procedure for assessment of significant gene expression ratios described below was also used for Northern blot data analysis.

Data Normalization and Transformation. The signals for replicate spots on one microarray were averaged. Following log-transformation, data were normalized using the mean of eight spiked mRNAs (Lucidea Universal Scorecard) selected in the linear segment of the "log(signal)/mRNA amount" curve.

Assessment of Significant Gene Expression Ratios. To assess the significance of gene expression ratios, we performed an analysis of variance (ANOVA) for each gene using the following model: log(normalized signal) = genotype + treatment + genotype:treatment + ε. We then performed multiple means comparisons using a two-tailed Student's test with a Bonferroni family-wise error rate protection (comparison-wise error rate set to 5% or 1%). By specifying the linear combinations of the ANOVA model factor levels, the number of comparisons was limited to the five meaningful comparisons presented and discussed in this article. Due to the Bonferroni correction, each ratio is declared significant if its raw p-value is $p < 0.002$ (for a 1% comparison-wise error rate) or $p < 0.01$ (for 5%). Because the number of genes is reduced (120 genes analyzed), the number of falsely significant ratios should not exceed 1.2. Results were further filtered by retaining solely the genes exhibiting at least one modulation exceeding an absolute 1.5-fold expression ratio between two groups and being highly significant (raw $p < 0.002$).

Multidimensional Statistical Analyses. For each organ, genes complying with the above criteria (at least one modulation with $p < 0.002$ and absolute ratio ≥1.5) were selected. Principal Component Analysis and hierarchical clustering were performed using this selection of scaled gene expression levels. The script used in this study (S-language) is available as supplemental material (http://www.inra.fr/Internet/Centres/toulouse/pharmacologie/pharmaco-moleculaire/valorisations/materiel.html).

RESULTS

Identification of Rexinoid-Regulated (LG100268) Murine Hepatic Transcripts by High-Density Microarray Screening

High-density screenings were performed to complement our literature mining efforts to document a relevant set of class II NR target genes. Here we present the results of the screening aimed at identifying RXR target genes in the liver. We selected the very specific and highly potent RXR activator, LG100268, and studied its effect on the liver transcriptome in wild-type mice. Pools of hepatic total RNA from three males treated with LG100268 (10 mg kg^{-1} day^{-1}, 8 days), or with the vehicle alone, were compared for transcript expression levels. Both cDNA samples were hybridized to a Mouse Unigene 1 glass slide (9596 IMAGE clones). As presented in Table 1, using the 1.7-fold cut-off value proposed by the manufacturer, we observed 44 upregulated transcripts (including six expressed sequences with no known function) and 27 downregulated transcripts (including one clone that does not belong to any Unigene cluster). Among the upregulated transcripts, 13 are unambiguously related to PPARα activation (Cyp4a14, bifunctional enzyme, Cyp4a10, Pdk4, cyclin D1, Slc22a5, SCD1, Crat, Facl2, Akp2, Acox1, Hmgcs 1, and Fabp1; full names appear in Table 1) and one (Cyp26a1) is a RAR target in mouse liver (22). Five downregulated transcripts are known PPARα targets (Mt 1 and 2, Gstp2, Mup1, Serpina1e) (9).

Development of a Customized Class II NR cDNA Macroarray: INRARRAY *01.2*

All available class II NR were identified from extensive literature screening and their corresponding

TABLE 1
LG100268-INDUCED HEPATIC GENE EXPRESSION MODULATIONS IN WILD-TYPE C57BL/6J MICE

Unigene Cluster Name	Clone Accession	Ratio
Genes induced by LG100268 in C57BL/6J mice		
Cyp4a14: cytochrome P450, family 4, subfamily a, polypeptide 14	AA106365	7.4
Ehhadh: enoyl-coenzyme A, hydratase/3-hydroxyacyl coenzyme A dehydrogenase	AA718155	6.5
Cyp4a10: cytochrome P450, family 4, subfamily a, polypeptide 10	AA755385	5.8
Cyp26a1: cytochrome P450, family 26, subfamily a, polypeptide 1	AA239785	5.4
G0s2: G0/G1 switch gene 2	AA458241	5.1
Pdk4: pyruvate dehydrogenase kinase, isoenzyme 4	AI322278	3.8
cDNA clone IMAGE: 5028619, partial cds	AI391013	3.1
Por: P450 (cytochrome) oxidoreductase	AI322279	2.7
Ccnd1: cyclin D1	AA117547	2.5
Alas1: aminolevulinic acid synthase 1	AI892379	2.3
Slc22a5: solute carrier family 22 (organic cation transporter), member 5	AI608375	2.2
Wbscr14: Williams-Beuren syndrome chromosome region 14 homolog (human)	AA543589	2.2
Sgk2: serum/glucocorticoid regulated kinase 2	AA138663	2.1
1700012B18Rik: RIKEN cDNA 1700012B18 gene	AI595047	2.0
Igfbp2: insulin-like growth factor binding protein 2	AA879643	2.0
Gadd45g: growth arrest and DNA-damage-inducible 45 gamma	W18822	2.0
Insig2: insulin-induced gene 2	AA197454	2.0
Scd1: stearoyl-coenzyme A desaturase 1	AA754922	1.9
Crat: carnitine acetyltransferase	AA473526	1.9
1500041J02Rik: RIKEN cDNA 1500041J02 gene	AI451818	1.8
Facl2: fatty acid coenzyme A ligase, long chain 2	AI789976	1.8
Akp2: alkaline phosphatase 2, liver	AA517588	1.8
Pla2g6: phospholipase A2, group VI	AA271866	1.8
Clu: clusterin	AA210481	1.8
5830435C13Rik: RIKEN cDNA 5830435C13 gene	AA200336	1.8
Cxadr: coxsackievirus and adenovirus receptor	AA560303	1.8
Adam11: A disintegrin and metalloprotease domain 11	AA733811	1.8
Aldh3a2: aldehyde dehydrogenase family 3, subfamily A2	AA821976	1.7
Acox1: acyl-coenzyme A oxidase 1, palmitoyl	AA612012	1.7
Scl27a2: solute carrier family 27 (fatty acid transporter), member 2	AA066694	1.7
Gadd45a: growth arrest and DNA-damage-inducible 45 alpha	AA553242	1.7
Crat: carnitine acetyltransferase	AI607260	1.7
AAss: aminoadipate-semialdehyde synthase	AA271121	1.7
Adfp: adipose differentiation related protein	AA624422	1.7
Gstt2: glutathione *S*-transferase, theta 2	AA511089	1.7
Hdc: histidine decarboxylase	AI322263	1.7
Cct2: chaperonin subunit 2 (beta)	W17932	1.7
Kap: kidney androgen regulated protein	AA106167	1.7
Transcribed sequences	AA242024	1.7
Vnn1: vanin 1	AI597120	1.7
Hsd17b9: hydroxysteroid (17-beta) dehydrogenase 9	AI425345	1.7
AW539457: expressed sequence AW539457	AI509582	1.7
Hmgcs1: 3-hydroxy-3-methylglutaryl-coenzyme A synthase 1	AA466979	1.7
Fabp1: fatty acid binding protein 1, liver	AI466451	1.7
Genes repressed by LG100268 in C57BL/6J mice		
Ppp1r3c: protein phosphatase 1, regulatory (inhibitor) subunit 3C	AA462037	−2.9
Mt2: metallothionein 2	W36474	−2.8
Trp53inp1: transformation related protein 53 inducible nuclear protein 1	AA437755	−2.6
Mt1: metallothionein 1	AA638765	−2.4
Rgs16: regulator of G-protein signaling 16	AA390086	−2.3
Sephs2: selenophosphate synthetase 2	AA414662	−2.1
Fos: FBJ osteosarcoma oncogene	AA002910	−2.1
Aqp1: aquaporin 1	AA241281	−2.0
Gstp2: glutathione *S*-transferase, pi 2	AA437941	−2.0
No Unigene cluster found	AI121690	−2.0
Got1: glutamate oxaloacetate transaminase 1, soluble	AA415254	−2.0
Similar to alpha-2u-globulin V precursor-mouse (LOC384025), mRNA	AA674270	−1.9
Cyp1a2: cytochrome P450, family 1, subfamily a, polypeptide 2	AA242360	−1.9
Rxra: retinoid X receptor alpha	AA462070	−1.9
Mup1: major urinary protein 1	AA822105	−1.8

TABLE 1
CONTINUED

Unigene Cluster Name	Clone Accession	Ratio
Serpina3c: serine (or cysteine) proteinase inhibitor, clade A, member 3C	W14912	−1.8
Idb2: inhibitor of DNA binding 2	AI322367	−1.8
Serpina1e: serine (or cysteine) proteinase inhibitor, clade A, member 1e	W13979	−1.8
Ela1: elastase 1, pancreatic	AA717025	−1.8
Dio1: deiodinase, iodothyronine, type I	AA260525	−1.7
Ell2: elongation factor RNA polymerase II 2	AA545429	−1.7
Cyp2a4: cytochrome P450, family 2, subfamily a, polypeptide 4	AA674177	−1.7
Acta1: actin, alpha 1, skeletal muscle	AA770902	−1.7
Acta2: actin, alpha 2, smooth muscle, aorta	AA624460	−1.7
Tdo2: tryptophan 2,3-dioxygenase	AA572623	−1.7
Cyp7a1: cytochrome P450, family 7, subfamily a, polypeptide 1	AI464796	−1,7
Sema4g: (semaphorin) 4G	AA238294	−1.7

Wild-type C57BL/6J mice were orally administered for 8 consecutive days 10 mg kg^{-1} day^{-1} of LG100268 or the vehicle alone ($n = 3$ per group). Hepatic total RNA were extracted. Pools of RNA corresponding to the treated and control groups were competitively hybridized to a mouse Unigene 1 microarray (Incyte Genomics, Inc., Palo Alto, CA, USA). Data are expressed as fold change (i.e., ratio of treated samples/control samples). Genes exhibiting an absolute expression ratio between the two groups superior to 1.7 are presented.

cDNA sequences were obtained from GenBank. For NR target genes identification, we relied on three independent data sources: i) published results from high-density screenings, ii) articles reporting gene regulation(s) by any of the class II NR activators, iii) our unpublished results of high-density screenings. The latter includes an additional study performed on Mouse Unigene 1 microarrays, with hepatic RNA from fenofibrate- or vehicle-treated mice of either wild-type (C57BL/6J) or PPARα-deficient genotype. Thus, we identified a set of PPARα-regulated hepatic transcripts (data not shown), which is largely redundant with the data obtained by Cherkaoui-Malki et al. [Unigene array (9)] and Yamazaki et al. [Affymetrix U74Av2 array (46)] both using the Wy14,643 PPARα-activator as a gene expression modulator.

Based on these data sources we developed a first version of a set of gene-specific probes (120 probes) relevant to the field of RXR and its known dimerization partners. We amplified these cDNAs from C57BL/6J mouse reverse transcribed RNAs (liver, kidney, enterocytes, adipose tissue, brain) using synthetic primers. All cDNAs were cloned into a common vector and all underwent a control procedure.

Due to the amount of available literature and to some of our sources (i.e., high-density screening with fibrate-treated livers) the PPARα signaling pathway holds a prevailing space within the array. The most represented genes belong to the following groups of functions: xenobiotic-metabolizing enzymes (phase I and phase II), ABC transporters, lipid homeostasis (synthesis, transport, catabolism), carbohydrates homeostasis (synthesis, storage, utilization).

INRA*RRAY* 01.2 was used to assess genes expression in liver, kidney, and heart of wild-type and PPARα –/– mice treated with fenofibrate, LGD1069, or vehicle alone. On the whole study (total of 72 macroarrays), the mean intragroup Pearson's correlation coefficient was 0.98 ± 0.01 (mean ± SD). Deviation from the ideal 1 value accounts for biological interindividual variability, technical variability, as well as presence of a few outlier macroarrays (3 out of 72 macroarrays); those values were subsequently removed from the datasets. Using artificial mRNAs spiked into the samples at known ratios between groups of mice, we showed that our macroarray data and subsequent analysis procedure led to reliable results as well as conservative estimations of expression ratios (Table 2). Theoretical 10-fold ratios appeared more affected by underestimation than threefold ratios, especially in the low intensity range (Table 2).

LGD1069 Induces a PPARα-Independent Hepatomegaly in Mice

Eight-month-old male C57BL/6J (wild-type) and PPARα –/– mice were orally treated for 8 consecutive days with fenofibrate (100 mg kg^{-1} day^{-1}), LGD1069 (100 mg kg^{-1} day^{-1}), or vehicle alone. Fenofibrate triggered a significant 47% increase in relative liver weight (liver weight/body weight, $p < 0.05$) in wild-type mice only. In contrast, the LGD1069-induced hepatomegaly observed in wild-type mice (30% increase, $p < 0.05$) was reproduced in PPARα –/– mice (22% increase, $p < 0.05$). Similarly, the treatment with LG100268 (10 mg kg^{-1} day^{-1}, 8 days), applied to wild-type mice, resulted in a significant hepatomegaly (27% increase, $p < 0.05$).

TABLE 2
THEORETICAL AND OBSERVED EXPRESSION RATIOS FOR EIGHT ARTIFICIAL mRNAs SPIKED INTO THE HEPATIC TOTAL RNA SAMPLES

Name	Intensity Range	Expected Ratio	Observed Ratio
Ratio 1	low	−3	−2.5 ± 0.4
Ratio 2	low	3	3.0 ± 0.8
Ratio 3	high	−3	−3.0 ± 0.6
Ratio 4	high	3	2.5 ± 0.3
Ratio 5	low	−10	−3.9 ± 0.8
Ratio 6	low	10	3.6 ± 0.6
Ratio 7	high	−10	−5.0 ± 0.5
Ratio 8	high	10	9.3 ± 1.4

Eight artificial mRNAs (Lucidea Universal ScoreCard, Amersham Biosciences, Orsay, France) were spiked into the RNA samples prior to labeling. These spikes were incorporated at known ratios between treated and control groups. Corresponding spots were arbitrarily divided as exhibiting a low (from 15 to 150 pg of spiked mRNA per sample) or high (from 500 to 5000 pg of spiked mRNA per sample) intensity. This table summarizes the expected and observed ratios (mean fold change ± SD) for the hybridization of hepatic RNAs from 24 mice. Similar results were obtained from the hybridizations of cardiac and renal samples (data not shown).

Effects of the Treatments on Serum Triglycerides, apoA-I, and apoB

The 8-month old PPARα-deficient mice displayed significantly higher constitutive serum triglycerides (112% increase, $p < 0.05$, $n = 5$ per genotype), apolipoprotein A-I (apoA-I, 20% increase, $p < 0.05$, $n =$ 14 or 15 per genotype), and apolipoprotein B (apoB, 84% increase, $p < 0.05$, $n = 14$ or 15 per genotype) levels compared to wild-type littermates. No effects of either LGD1069 or fenofibrate were observed on serum triglycerides (TG) in PPARα –/– mice. In contrast, LGD1069 induced a significant 76% increase in serum TG of wild-type mice ($p < 0.05$, $n = 5$ per group). Although nonsignificant in this study, we noticed a 20% decrease of the mean serum TG in wild-type mice treated with fenofibrate. No significant effects of the treatments were observed on serum apoA-I and apoB.

Hepatic, Renal, and Cardiac Effects of LGD1069 and Fenofibrate on the Abundance of a Selection of Class II NR-Related Transcripts in Wild-Type and PPARα-Deficient Mice

We used INRA*RRAY* 01.2 to screen the effects of LGD1069 and fenofibrate on our selected genes panel in wild-type and PPARα-deficient mice liver, kidney, and heart. Significantly modulated genes were identified as described in the Materials and Methods.

As shown in Table 3, using this procedure with a 1% comparison-wise error rate we identified in wild-type mice liver 14 genes significantly modulated by LGD1069 treatment (11 upregulated and 3 downregulated) and 24 genes significantly modulated by fenofibrate treatment (21 upregulated and 3 downregulated). In PPARα-deficient mice liver, LGD1069 treatment significantly increased the level of five transcripts and fenofibrate treatment of one transcript. Furthermore, three transcripts showed significantly higher levels and one transcript a lower level in PPARα –/– mice compared to wild-type mice under the control treatment.

In wild-type mice kidney (Table 4), LGD1069 significantly increased the levels of 15 transcripts while fenofibrate significantly increased the levels of 17 transcripts. In PPARα-deficient mice kidney, LGD1069 significantly upregulated the cytochromes P450 24 and 27b1 as found in wild-type mice but also induced apoE mRNA expression. Fenofibrate did not trigger any significant modulations in PPARα –/– mice kidney. Fourteen transcripts were found differentially expressed between control wild-type and PPARα –/– mice kidney (eight transcripts overexpressed and six transcripts underexpressed in PPARα –/– mice kidney compared to wild-type littermates).

Screening of wild-type and PPARα –/– mice heart under vehicle, fenofibrate, or LGD1069 treatment led to a more limited number of significant gene expression modulations. Under the control treatment, the pyruvate dehydrogenase kinase 4 (PDK4), the peroxisomal/mitochondrial dienoyl-CoA isomerase (PMDCI), as well as both subunits of the mitochondrial hydroxyacyl-CoA dehydrogenase/3-ketoacyl-CoA thiolase/enoyl-CoA hydratase trifunctional protein (Tpα and Tpβ), were downregulated in PPARα –/– mice compared to wild-type mice heart (−2.2-, −2.9-, −1.6-, and −1.7-fold, respectively, all $p < 0.002$). The only significant regulation triggered by the treatments was the induction of PDK4 mRNA level under LGD1069 treatment. This upregulation was found significant in wild-type (2.4-fold, $p < 0.002$) and in PPARα –/– mice (3.3-fold, $p < 0.002$) as previously reported (35).

Northern Blot Analysis of Some Gene Expression Modulations

To confirm some of these gene expression regulations, Northern blots of individual mRNA samples were performed (Figs. 1, 2, and 3). In the liver (Fig. 1), except for Cyp8b1, all regulations observed by Northern blot are in agreement with the macroarray results. Macroarrays as well as Northern blot identified a modestly significant upregulation of Cyp8b1 by fenofibrate (1.8-fold and 2.3-fold, respectively, both $p < 0.01$) in wild-type mice only. While Northern blot data indicated a significant downregulation

TABLE 3
HEPATIC GENE EXPRESSION MODULATIONS INDUCED BY FENOFIBRATE OR LGD1069 IN WILD-TYPE AND PPARα –/– MICE

Genes	Wild-Type		PPARα –/–		CT PPARα –/–/wt	Function
	Feno/CT	LGD1069/CT	Feno/CT	LGD1069/CT		
Cyp4a10	32.9†	7.8†	ns	ns	ns	microsomal FA ω-hydroxylation
Cyp4a14	44.8†	12.0†	ns	ns	2.4†	microsomal FA ω-hydroxylation
AOX	6.4†	2.5†	ns	ns	ns	peroxisomal FA oxidation and biogenesis
BIEN	40.0†	5.1†	ns	ns	ns	peroxisomal FA oxidation and biogenesis
THIOL	8.5†	3.8†	ns	ns	ns	peroxisomal FA oxidation and biogenesis
PECI	2.1†	ns	ns	ns	ns	peroxisomal FA oxidation and biogenesis
PMDCI	3.2†	ns	ns	ns	ns	peroxisomal FA oxidation and biogenesis
Pex11a	2.1†	ns	ns	ns	ns	peroxisomal FA oxidation and biogenesis
CACP	1.8†	ns	ns	ns	ns	mitochondrial FA oxidation and energy homeostasis
CPT2	1.7†	ns	ns	ns	ns	mitochondrial FA oxidation and energy homeostasis
MCAD	2.8†	ns	ns	ns	1.6*	mitochondrial FA oxidation and energy homeostasis
Tpα	2.4†	ns	ns	ns	ns	mitochondrial FA oxidation and energy homeostasis
mHMGCoAS	3.1†	1.5*	ns	ns	ns	mitochondrial FA oxidation and energy homeostasis
PDK4	3.3†	ns	ns	ns	ns	mitochondrial FA oxidation and energy homeostasis
ACOTH	6.3†	2.0*	ns	ns	ns	FA metabolism
FAT/CD36	1.9†	ns	ns	ns	ns	FA transport
L-FABP	4.2†	ns	ns	ns	ns	FA trafficking
FAS	ns	3.5†	ns	2.4†	ns	lipogenesis
S14	ns	2.4†	ns	ns	ns	lipogenesis
Cyp26	ns	3.5†	ns	4.4†	ns	other cytochromes P450
Cyp2b10	ns	4.6†	1.7†	3.3†	ns	other cytochromes P450
Cyp2c29	–1.6†	2.2†	ns	1.7†	1.5†	other cytochromes P450
Cyp8b1	1.8*	–2.1†	ns	ns	ns	other cytochromes P450
ALDH3	4.1†	ns	ns	ns	ns	fatty aldehyde dehydrogenase
GSTμ	ns	2.2†	ns	ns	ns	glutathione *S*-transferases
GSTπ2	ns	–3.6†	ns	ns	–2.9†	glutathione *S*-transferases
LCE	–1.6†	ns	ns	ns	ns	TG hydrolysis
PLTP	2.0†	ns	ns	ns	ns	lipoprotein metabolism
apoC-III	ns	ns	ns	ns	1.6†	lipoprotein metabolism
PPARα	1.6†	ns	ns	ns	ns	nuclear receptor
SPI1	–2.7†	–2.1†	ns	–1.6*	–1.6*	acute phase response
ADISP/FSP27	2.0†	ns	ns	ns	ns	apoptosis
BSEP	ns	ns	ns	1.9†	ns	bile salt transport

Hepatic total RNA from wild-type and PPARα –/– mice treated with fenofibrate (Feno), LGD1069, or vehicle alone (CT) were hybridized to INR*ARRAY* 01.2 ($n = 3$ or 4 per group, total of 22 macroarrays). Raw data were normalized by the mean log(signal) of eight artificial mRNAs spiked into the samples. Normalized data were subjected to an ANOVA followed by a two-tailed Student's test using a Bonferroni comparison-wise error rate protection. The ratios (fold change) of transcript abundance correspond to the comparisons between the groups indicated in the headings of the columns. Genes presented exhibited at least one highly significant ($p < 0.002$) gene expression modulation of 1.5-fold amplitude minimum out of the five comparisons studied. wt: wild-type.
Due to the Bonferroni p-value adjustments: *raw $p < 0.01$ and †raw $p < 0.002$. ns: a nonsignificant expression ratio (raw $p > 0.01$).

of Cyp8b1 mRNA by LGD1069 only in PPARα –/– mice (–2.5-fold, $p < 0.002$), macroarrays did not find this regulation significant (–1.3-fold, $p > 0.01$). Conversely, macroarrays identified a significant LGD1069-induced downregulation of Cyp8b1 only in wild-type mice (–2.1-fold, $p < 0.002$). Although suggesting the same trend, this downregulation was not found significant by Northern blot (–1.9-fold, $p > 0.01$). We thus confirmed the PPARα-independent regulations of Cyp2c29, Cyp26, Cyp2b10, FAS (all upregulated), and SPI1 (downregulated) mRNAs by LGD1069. In PPARα –/– mice liver compared to wild-type littermates, the constitutive underexpression of GSTπ2 and SPI1 mRNAs as well as a modest overexpression

TABLE 4
RENAL GENE EXPRESSION MODULATIONS INDUCED BY FENOFIBRATE OR LGD1069 IN WILD-TYPE AND PPARα –/– MICE

	Wild-Type		PPARα –/–			
Genes	Feno/CT	LGD1069/CT	Feno/CT	LGD1069/CT	CT PPARα –/–/wt	Function
Cyp4a10	5.5†	2.8†	ns	ns	−2.4†	microsomal FA ω-hydroxylation
Cyp4a14	22.1†	7.7†	ns	ns	ns	microsomal FA ω-hydroxylation
AOX	2.1†	1.7†	ns	ns	ns	peroxisomal FA oxidation and biogenesis
BIEN	5.0†	2.1†	ns	1.5*	−2.0†	peroxisomal FA oxidation and biogenesis
THIOL	3.0†	2.4†	ns	ns	ns	peroxisomal FA oxidation and biogenesis
PECI	1.6†	1.6†	ns	ns	ns	peroxisomal FA oxidation and biogenesis
PMDCI	1.9†	ns	ns	ns	−1.8†	peroxisomal FA oxidation and biogenesis
HPNCL	2.2†	1.8†	ns	ns	ns	peroxisomal FA oxidation and biogenesis
Pex11a	2.0†	ns	ns	ns	ns	peroxisomal FA oxidation and biogenesis
CACP	1.8†	1.3†	ns	ns	ns	mitochondrial FA oxidation and energy homeostasis
CPT2	2.1†	1.5†	ns	ns	−1.3*	mitochondrial FA oxidation and energy homeostasis
Tpα	1.6†	1.2*	ns	ns	ns	mitochondrial FA oxidation and energy homeostasis
mHMGCoAS	10.4†	3.7†	ns	ns	ns	mitochondrial FA oxidation and energy homeostasis
PDK4	5.6†	3.1†	ns	ns	ns	mitochondrial FA oxidation and energy homeostasis
UCP2	3.8†	1.6†	ns	ns	ns	mitochondrial FA oxidation and energy homeostasis
ACOTH	4.6†	2.9†	ns	ns	ns	FA metabolism
L-FABP	2.1†	1.3*	ns	ns	1.4†	FA trafficking
Cyp24	ns	3.2†	ns	1.9†	2.2†	other cytochromes P450
Cyp27b1	ns	2.6†	ns	1.9†	2.1†	other cytochromes P450
Cyp2c29	ns	ns	ns	−1.7*	2.0†	other cytochromes P450
LPL	−1.6*	ns	ns	ns	−1.8†	TG hydrolysis
apoB	ns	ns	ns	ns	1.7†	lipoprotein metabolism
apoE	ns	ns	ns	2.9†	2.0†	lipoprotein metabolism
CAR1	ns	ns	ns	ns	1.6†	nuclear receptor
SPI1	ns	ns	ns	ns	−1.9†	acute phase response
i-NOS	1.4*	ns	ns	ns	1.6†	inflammation
cHMGCoAS	ns	ns	ns	ns	−2.1†	cholesterol biosynthesis

Renal total RNA from wild-type and PPARα –/– mice treated with fenofibrate (Feno), LGD1069, or vehicle alone (CT) were hybridized to INRA*RRAY* 01.2 ($n = 3$ or 4 per group, total of 23 macroarrays). Raw data were normalized by the mean log(signal) of eight artificial mRNAs spiked into the samples. Normalized data were subjected to an ANOVA followed by a two-tailed Student's test using a Bonferroni comparison-wise error rate protection. The ratios (fold change) of transcript abundance correspond to the comparisons between the groups indicated in the headings of the columns. Genes presented exhibited at least one highly significant ($p < 0.002$) gene expression modulation of 1.5-fold amplitude minimum out of the five comparisons studied. wt: wild-type.
Due to the Bonferroni p-value adjustment: *raw $p < 0.01$ and †raw $p < 0.002$. ns: a nonsignificant expression ratio (raw $p > 0.01$).

of Cyp2c29 mRNA were also confirmed. PPARα-dependent downregulation of Cyp2c29 and SPI1 by fenofibrate was also found by both techniques. We observed that fenofibrate raised the hepatic expression of Cyp2b10 transcript in PPARα –/– mice only, with a noticeable interindividual variability of the response to the drug.

In the kidney (Fig. 2), we confirmed the constitutive overexpression of Cyp24 and Cyp27b1 in PPARα –/– mice compared to wild-type mice. LGD1069 induced in both PPARα –/– and wild-type mice kidney an upregulation of these two genes. As shown in Figure 3, we further confirmed that PPARα –/– mice slightly overexpressed apoE mRNA in the absence of LGD1069 or fenofibrate treatments. A very modest downregulation of renal apoE mRNA was observed in wild-type mice under fenofibrate treatment. We clearly identified that LGD1069 strongly induced the expression of renal apoE mRNA in PPARα –/– mice only (Fig. 3).

Principal Component Analysis (PCA) of Hepatic and Renal Dedicated Transcriptional Signatures

To globally represent the transcriptional signatures obtained in the liver and the kidney, we used PCA

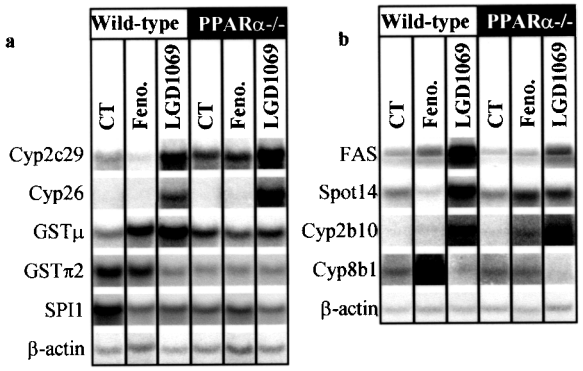

c

	Wild-type		PPARα-/-		CT
	Feno. / CT	LGD / CT	Feno. / CT	LGD / CT	PPARα -/- / wt
Cyp2c29	-1.6**	3.0**	ns	1.7**	1.5*
Cyp26	ns	31**	ns	14**	ns
GSTμ	ns	3.4**	ns	ns	ns
GSTπ2	ns	-3.7**	ns	ns	-4.2**
SPI1	-2.6**	-1.7**	ns	-1.6*	-1.9**
FAS	ns	3.8**	ns	2.6*	ns
Spot14	ns	7.6**	ns	ns	ns
Cyp2b10	ns	36.3**	4.6*	12.7**	ns
Cyp8b1	2.3*	ns	ns	-2.5**	ns

Figure 1. Regulation of transcript abundance in the liver of wild-type and PPARα–/– mice by LGD1069 and fenofibrate. Northern blot analyses were carried out using 20 μg of hepatic total RNA per lane. cDNA fragments spotted on the INRA*RRAY* 01.2 were used as [α-^{32}P]dCTP-labeled probes. Samples from three animals were analyzed for each condition ($n = 3 \times 6$ experimental conditions = 18 samples). (a, b) The results of 11 different hybridizations are presented (6 and 5 for a and b, respectively). Pictures obtained for 6 liver samples representative of the 6 groups of samples analyzed are presented. (c) Isotopic signals were quantified for the full set of 18 samples using a phosphorimager. Raw data generated for each gene were normalized according to the corresponding β-actin hybridization data. Normalized data were subjected to an ANOVA followed by a two-tailed Student's test using a Bonferroni comparison-wise error rate protection. The ratios of transcript abundance between the groups are indicated in the headings of the columns. Due to the Bonferroni p-value adjustments, *raw $p < 0.01$ and **raw $p < 0.002$. ns: a nonsignificant expression ratio (raw $p > 0.01$). CT: vehicle-treated control group, LGD: LGD1069, Feno.: fenofibrate.

on the subset of scaled variables presented in Tables 3 and 4 (33 and 27 selected genes for liver and kidney, respectively). Figure 4 presents the first three principal components obtained for the kidney. Very similar results were obtained for the liver and are thus not presented in this article. PCA allowed us to observe the hierarchy of variability sources affecting the transcriptional signatures. The biological meaning of these variability sources was extracted from the projections of the genes on the principal components (Fig. 4b and d). Figure 4a corresponds to the projection of the mice on the first two principal components (PC1 and PC2), which extracted 57% and 20% of the total variability of the initial dataset, respectively. Wild-type mice treated with fenofibrate were markedly separated from wild-type controls along PC1 (Fig. 4a). All LGD1069-treated wild-type mice adopted an intermediate position along this axis. The three groups of PPARα –/– mice were not separated along PC1. A majority of the 27 genes were highly correlated to PC1 (Fig. 4b). These genes are mostly well-described PPARα-target genes implicated in various steps and pathways of fatty acid catabolism. PC2 discriminated all groups of PPARα –/– mice from wild-type controls. This axis was most highly correlated with genes displaying a constitutive differential expression between wild-type and PPARα –/– mice (Fig. 4b, Table 4, fifth column) such as inducible nitric oxide synthase (i-NOS), constitutive androstane receptor β (CAR1), or lipoprotein lipase (LPL). The third axis (PC3), which is orthogonal to PC1 and PC2, discriminated LGD1069-treated mice of both genotypes from

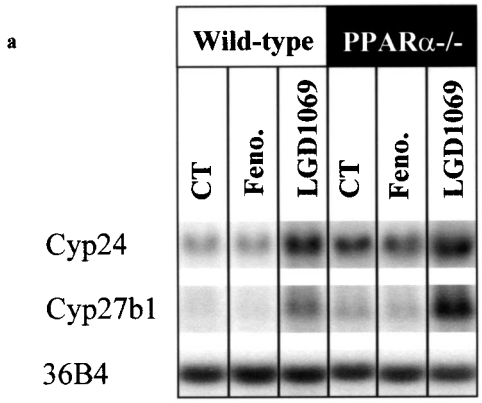

b

	Wild-type		PPARα-/-		CT
	Feno. / CT	LGD / CT	Feno. / CT	LGD / CT	PPARα -/- / wt
Cyp24	ns	3.6**	ns	1.8**	2.9**
Cyp27b1	ns	3.9**	ns	3.1**	2.7**

Figure 2. Regulation of Cyp24 and Cyp27b1 transcript abundance in the kidney of wild-type and PPARα–/– mice by LGD1069 and fenofibrate. The experimental conditions for these Northern blot analyses are identical to those described in the legend of Figure 1, except for the number of animals per experimental group ($n = 4 \times 6$ experimental conditions = 24 samples). (a) The results of three different hybridizations are presented. Pictures obtained for 6 liver samples representative of the 6 groups of samples analyzed are presented. (b) Isotopic signals were quantified for the full set of 24 samples using a phosphorimager. Raw data generated for each gene were normalized according to the corresponding 36B4-probe hybridization data. Normalized data were subjected to an ANOVA followed by a two-tailed Student's test using a Bonferroni comparison-wise error rate protection. (b) The ratios of transcript abundance between the groups are indicated in the headings of the columns. Due to the Bonferroni p-value adjustments: *raw $p < 0.01$ and **raw $p < 0.002$. ns: a nonsignificant expression ratio (raw $p > 0.01$). CT: vehicle-treated control group, LGD: LGD1069, Feno.: fenofibrate.

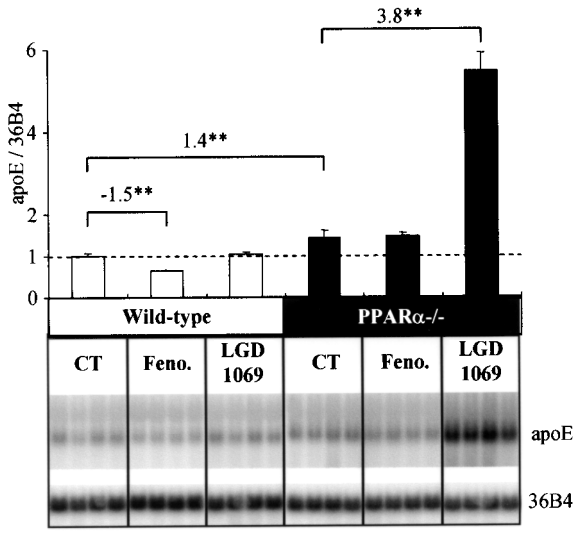

Figure 3. Regulation of apoE transcript abundance in the kidney of wild-type and PPARα–/– mice by LGD1069 and fenofibrate. The experimental conditions for these Northern blot analyses are identical to those described in the legend of Figure 2. The pictures corresponding to all 24 kidney samples hybridized with apoE or 36B4 radiolabeled probes are presented in the lower part. Isotopic signals were quantified for the full set of 24 samples using a phosphorimager. Raw data generated for apoE mRNA were normalized according to the corresponding 36B4-probe hybridization data. Normalized data were subjected to an ANOVA followed by a two-tailed Student's test using a Bonferroni comparison-wise error rate protection. Histograms represent the mean of normalized data for each of the 6 experimental conditions, compared to the group of control (CT) wild-type mice. Error bars represent SD. Lines above the bars indicate which comparisons gave significant results. Expression ratios (or fold change) are given above these lines. Due to the Bonferroni p-value adjustments: **raw $p < 0.002$. CT: vehicle-treated control group, Feno.: fenofibrate.

all other mice (Fig. 4c). This axis was most highly correlated with cytochromes P450 (Cyp) 24, 27b1, and 2c29 and to a lesser extent to apoE.

DISCUSSION

Several class II NR display a valuable potential as they behave as drug sensors. Through their control on gene expression, they convey the beneficial effects of drugs that prove to be active on dyslipidemia, diabetes, or skin disorders. The lately developed drug family, rexinoids, is unique in that its members selectively activate RXR, the obligatory partner for all class II NRs. Activation of this central communication node could potentially result in modulations of various pathways through differential recruitment of dimeric partners. Thus, multiorgan screening of gene expression modulations is a relevant strategy to anticipate and delineate the tissue-specific pharmacological and/or toxicological impacts of rexinoids. Therefore, we designed and developed a dedicated cDNA macroarray to implement this study. Our primary motivation was to record true organ-specific "fingerprints" of NR targeting drugs that contribute to accurately reporting their molecular impact on a mammalian organism. Remarkably, this allows considering global sets of data that include all statistically significant transcript modulations, even those displaying weak magnitude and, thus, doubtful biochemical significance when considered individually. Indeed, all these limited regulations retain, and even gain, significance when they are processed as multivariate signatures and when they are analyzed through multidimentional statistical methods such as PCA or hierarchical clustering. We believe that improving the accuracy of organ-specific transcriptional signatures is a relevant mean to focus, secondarily, the investigations on pathways where protein levels are eligible to fluctuate in response to NR activators, although this was not the aim of this initial investigation.

Hepatic and Renal Transcriptional Signatures Analysis

PCA was used to observe the main effects of the treatments and of PPARα deletion on the transcriptional signatures. Renal (Fig. 4) and hepatic (data not shown) transcriptional signatures displayed comparable patterns. The first PC was strongly correlated to numerous genes regulated by LGD1069 and fenofibrate in wild-type mice only and should thus be regarded as the illustration of PPARα-dependent effects of the treatments on gene expression. The intermediate position of wild-type LGD1069-treated mice on this axis revealed the lower activation of the PPARα signaling pathway by LGD1069 compared to fenofibrate. The second PC highlighted the importance of renal constitutive gene expression alterations following PPARα abrogation. Finally, PC3 should be predominantly interpreted as PPARα-independent effects of LGD1069 on Cyp24 and Cyp27b1 expressions. Hierarchical clustering of both genes and samples was also used to analyze these data and led to similar conclusions (data not shown).

Rexinoid-Induced Hypertriglyceridemia

Although conflicting data have been collated in rodents (35), oral treatment with rexinoids can induce hypertriglyceridemia in humans (39). As previously presented, such hypertriglyceridemia can be observed in PPARα –/– mice younger than those monitored in the present study (35). Using 8-month-old animals, a significant rise in serum TG was only observed in wild-type mice. At the molecular level, our data indicate that LGD1069 treatment raises the level of two transcripts related to fatty acid synthesis: Spot14

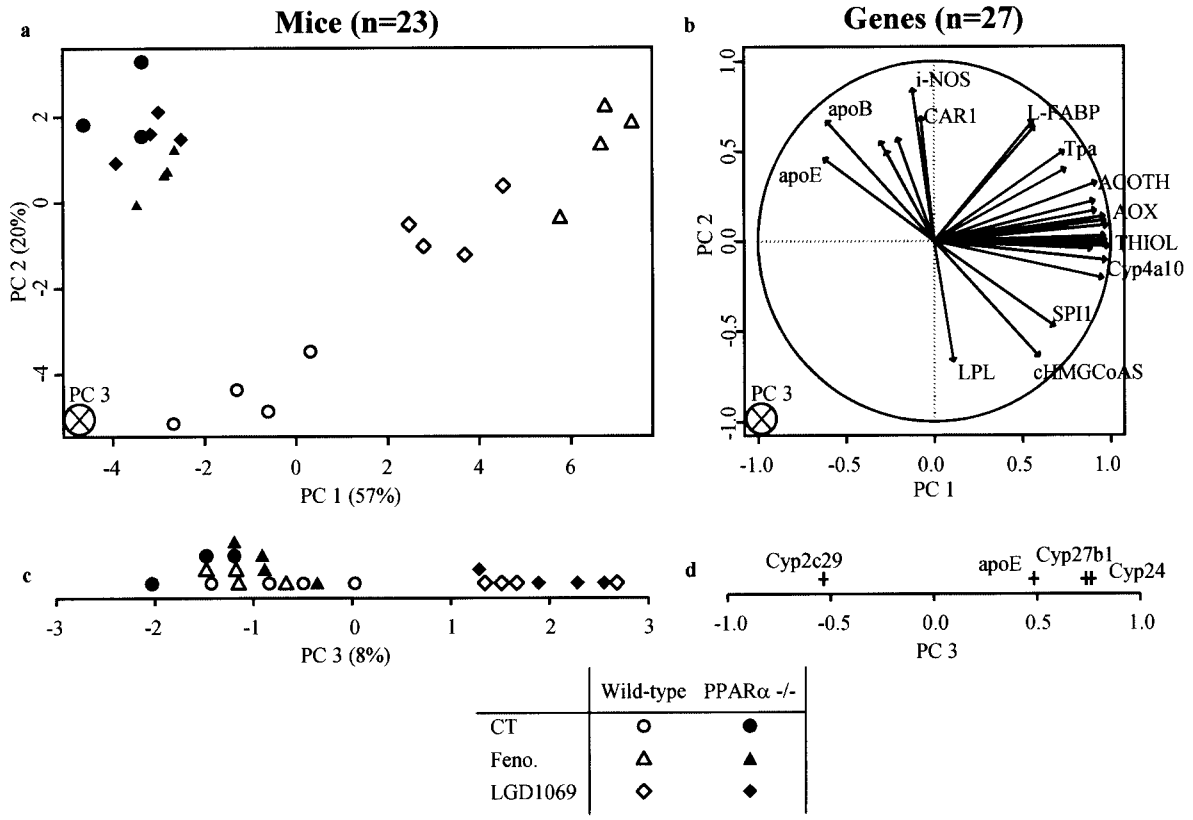

Figure 4. Principal component analysis of renal transcriptional signatures of wild-type and PPARα –/– treated with LGD1069, fenofibrate, or vehicle alone. Principal component analysis was performed on a data matrix composed of 23 RNA samples (mice) and 27 selected genes presented in Table 4. Thus, only one macroarray, corresponding to one PPARα –/– control mouse, was identified as outlier by quality controls and removed from the data set. (a) Plot of the 23 samples (mice) on the first two principal components (PC). Numbers in parentheses indicate the percentage of the total variance extracted by the corresponding PC. Open symbols correspond to wild-type mice and filled symbols to PPARα –/– mice. Circles are for controls (CT), diamonds for LGD1069-treated, and triangles for fenofibrate-treated (Feno.) mice. (b) Plot of genes (variables) on the first two PC. Each vector represents one gene. The names of some genes have been removed to facilitate the reading of the figure. (c) Plot of the 23 samples on the third PC. Points having close coordinates on this axis were piled up to facilitate the reading. (d) Plot of the genes on the third axis. Each gene's coordinate is represented by a cross. Only the four genes whose coordinates on the third PC were superior to 0.4 are represented. The names of the corresponding genes are indicated.

(S14) and fatty acid synthase (FAS) in wild-type mice. Although to a lesser extent, the rise of FAS mRNA is partially sustained in PPARα –/– mice. Furthermore, our data evidenced a 1.9-fold rise of Stearoyl-CoA desaturase 1 mRNA in wild-type mice following LG100268 treatment (Table 1). Altogether, these observations are consistent with a coordinated action of rexinoids on a set of genes known to promote hypertriglyceridemia. Based on our findings, it would be of great interest to assess the putative roles played by known lipogenesis regulators (e.g., SREBP, TR, or LXR) in this phenomenon, which could be related to a documented side effect of rexinoids.

Organ-Specific Rexinoid Targets

Besides renal and hepatic PPARα activation illustrated by PCA, we observed a more restricted number of PPARα-independent gene expression modulations. In liver, LGD1069 induces Cyp2b10, a known target for PXR and CARβ. The tandem DR-4 element from mouse Cyp2b10 does not respond to LGD1069 in RXR and/or CARβ-transfected HepG2 cells (41). However, this cannot rule out the putative involvement of CARβ nor of PXR in the context of our in vivo study (44). In addition, Cyp2c29 is also induced by LGD1069 in a PPARα-independent manner and has recently been shown to be a target of CARβ (20). Of interest is our original observation of the marked rise in hepatic Cyp26 transcript by both rexinoid molecules. Besides its role in the degradative 4-hydroxylation of *all-trans* RA during embryonic development (1,34), Cyp26 is thought to participate in limiting the access of RA to the transcriptional machinery (27). Regulation of Cyp26 by *all-trans* RA has been extensively studied (29,45). The central role RARγ and

RXRα has first been delineated using modified murine F9 cells lacking retinoid receptors (2). Cell line-specific interactions between a RA-response element (RARE-DR5) and other Cyp26 promoter regions have been shown (26). Here, we provide the first evidence that hepatic Cyp26 transcript can be upregulated in vivo by highly specific RXR activators. Even partially translated to the protein level, such a marked induction could have a profound repercussion on the cellular bioavailability of RA, thus possibly hampering the activity of the RXR–RAR dimer.

Very interestingly, in the kidney, we observed a significant induction by LGD1069 of Cyp24 and Cyp27b1, whose products are involved in vitamin D_3 homeostasis. Although constitutively overexpressed in PPARα –/– mice, these two genes are still responsive to LGD1069 treatment in this mouse model. Cyp24 and Cyp27b1 encode a 25-hydroxyvitamin D_3 24-hydroxylase (19) and a 25-hydroxyvitamin D_3 1α-hydroxylase (40), respectively. These enzymes display opposite biosynthetic (Cyp27b1) and catabolic (Cyp24) functions in the homeostasis of the active form of vitamin D_3 (1α,25-dihydroxyvitamin D_3). Induction of Cyp24 transcript in mouse kidney by LG100268 has been previously shown (3). In humans, this induction is mediated by RXR–RAR or RXR–VDR heterodimers binding on two vitamin D-responsive elements (VDREs) located in the promoter of CYP24 (47). Recently, Pascussi et al. identified PXR as a novel transcriptional regulator of both mouse and human Cyp24 (36), thus providing an additional mechanistic hypothesis for the regulation that we observed. Cyp27b1 was shown to be downregulated by liganded VDR (40). Here we show that both Cyp24 and Cyp27b1 are induced to a similar extent by LGD1069 in mouse kidney, independently of PPARα expression. Consistent with a previously documented rexinoid-induced expression of Cyp24, we could hypothesized that a subsequent renal depletion in active vitamin D derivative would lower the activated proportion of the VDR, thus allowing the upregulation of Cyp27b1 reported here. However, this hypothesis remains to be fully substantiated. The coordinated modulation of two genes oppositely associated to the bioavailability of cellular active vitamin D suggests the existence of a putative feedback loop that could preserve a physiological balance between active and inactive vitamin D metabolites. Interestingly, our study revealed that Cyp27b1 is a novel target for the rexinoid family of xenobiotics, which likely deserves future attention in the skin.

The RXR–RAR, RXR–TR, and RXR–VDR dimers were initially reported to be nonpermissive (14). Consistent observations now support the concept that upon specific activation, RXR could become an active contributor to gene expression modulation. Its action towards RAR, TR, or VDR known target genes appears subordinated to favorable cellular conditions that affect its partner (4,18,25,30). Further evidences, consistent with this concept, are provided by our in vivo studies. Indeed, the nature of the rexinoid-modulated targets indicate that various signaling pathways deserve further detailed investigations (e.g., RAR and CARβ in the liver and VDR in the kidney). In general, this illustrates how cautiously the concept of dimer permissiveness should be viewed and how much it is likely to rely on specific experimental conditions.

This study further identified a puzzling regulation of the renal apolipoprotein E (apoE) transcript. ApoE is a surface constituent of plasma lipoproteins and a high-affinity ligand for the LDL receptor, which mediates the hepatic uptake of remnant lipoproteins. Although mostly produced in the liver, plasma apoE is also synthesized in various extrahepatic tissues including kidney (5,38). Strikingly, renal apoE mRNA is strongly induced by LGD1069 in PPARα –/– mice only. Response elements for LXRs (21) and PPARs (16) have been found in apoE promoter. Our observations suggest that the PPARα signaling pathway exerts an inhibitory control over renal apoE transcription through a direct or indirect mechanism that remains to be described. Furthermore, besides its clear atheroprotective effects through lipoprotein metabolism control, apoE displays antiproliferative functions in kidney (8) and most interestingly in mitogen-activated T lymphocytes (31), as in endothelial and tumor cells (42). Our work showed that LGD1069 has a capacity to regulate, in vivo, the apoE transcript as LG100268 does on the human THP-1 monocytic/macrophage line (21). Thus, we observed a degree of consistency between the pharmacological ability of rexinoids to limit cell proliferation in lymphoproliferative disorders and their potential to regulate the expression of apoE, an antiproliferative mediator. Exploring hypothetical causal links between these observations might represent a promising strategy to further elucidate the molecular events lying behind the beneficial effects of rexinoids in CTCL patients.

Together our results suggest that the PPARα signaling pathway is the most sensitive pathway to be recruited through specific ligand activation of RXR in liver and kidney. However, the identification of several organ-specific, PPARα-independent modulations triggered by LGD1069 suggests that different cellular contexts are capable of eliciting partial but active contributions of various NR signaling pathways.

The development of a dedicated set of target genes to study the organ-specific transcriptional signature

of rexinoids has documented the complex nature of their molecular impact in vivo. Although the development state of our dedicated macroarray does not yet allow us to fully explore all class II NR pathways, we show that this strategy already provides interesting evidences that rexinoids affect different molecular pathways in an organ-specific manner. These signatures strongly suggest that rexinoids trigger a sophisticated interplay between several NR signaling pathways. Further investigations are required to precisely delineate this network. Ongoing developments of our macroarray and its use in several organs and chemical exposure conditions will provide an additional valuable tool to improve our understanding of the pathways followed by drugs, pollutants, nutrients, or hormones to sustain their biological actions.

ACKNOWLEDGMENTS

We are indebted to L. Ouamrane-Bernard (Galderma-Inra CIFRE-PhD program) for her expertise in triglycerides and lipoprotein analysis in mice and for monitoring the commercial microarray screening. We thank C. Bétoulières, G. Galy, and A.-M. Caussalter for excellent technical assistance. We are grateful to Dr. F. J. Gonzalez for the generous gift of the PPARα –/– mouse line. P. G. P. Martin was supported by the Ligue contre le cancer and A. Roulet by the Association pour la Recherche contre le Cancer. This work was supported by a grant from the ATC Nutrition founded by INSERM and INRA (AIP275) and by a grant from the Agence Française de Sécurité Sanitaire de l'Environnement (RD-2003-018/A2049).

REFERENCES

1. Abu-Abed, S.; Dolle, P.; Metzger, D.; Beckett, B.; Chambon, P.; Petkovich, M. The retinoic acid-metabolizing enzyme, CYP26A1, is essential for normal hindbrain patterning, vertebral identity, and development of posterior structures. Genes Dev. 15:226–240; 2001.
2. Abu-Abed, S. S.; Beckett, B. R.; Chiba, H.; Chithalen, J. V.; Jones, G.; Metzger, D.; Chambon, P.; Petkovich, M. Mouse P450RAI (CYP26) expression and retinoic acid-inducible retinoic acid metabolism in F9 cells are regulated by retinoic acid receptor gamma and retinoid X receptor alpha. J. Biol. Chem. 273:2409–2415; 1998.
3. Allegretto, E. A.; Shevde, N.; Zou, A.; Howell, S. R.; Boehm, M. F.; Hollis, B. W.; Pike, J. W. Retinoid X receptor acts as a hormone receptor in vivo to induce a key metabolic enzyme for 1,25-dihydroxyvitamin D3. J. Biol. Chem. 270:23906–23909; 1995.
4. Bettoun, D. J.; Burris, T. P.; Houck, K. A.; Buck, D. W., 2nd; Stayrook, K. R.; Khalifa, B.; Lu, J.; Chin, W. W.; Nagpal, S. Retinoid X receptor is a nonsilent major contributor to vitamin D receptor-mediated transcriptional activation. Mol. Endocrinol. 17:2320–2328; 2003.
5. Blue, M. L.; Williams, D. L.; Zucker, S.; Khan, S. A.; Blum, C. B. Apolipoprotein E synthesis in human kidney, adrenal gland, and liver. Proc. Natl. Acad. Sci. USA 80:283–287; 1983.
6. Boehm, M. F.; Zhang, L.; Badea, B. A.; White, S. K.; Mais, D. E.; Berger, E.; Suto, C. M.; Goldman, M. E.; Heyman, R. A. Synthesis and structure–activity relationships of novel retinoid X receptor-selective retinoids. J. Med. Chem. 37:2930–2941; 1994.
7. Boehm, M. F.; Zhang, L.; Zhi, L.; McClurg, M. R.; Berger, E.; Wagoner, M.; Mais, D. E.; Suto, C. M.; Davies, J. A.; Heyman, R. A.; et al. Design and synthesis of potent retinoid X receptor selective ligands that induce apoptosis in leukemia cells. J. Med. Chem. 38: 3146–3155; 1995.
8. Chen, G.; Paka, L.; Kako, Y.; Singhal, P.; Duan, W.; Pillarisetti, S. A protective role for kidney apolipoprotein E. Regulation of mesangial cell proliferation and matrix expansion. J. Biol. Chem. 276:49142–49147; 2001.
9. Cherkaoui-Malki, M.; Meyer, K.; Cao, W. Q.; Latruffe, N.; Yeldandi, A. V.; Rao, M. S.; Bradfield, C. A.; Reddy, J. K. Identification of novel peroxisome proliferator-activated receptor alpha (PPARalpha) target genes in mouse liver using cDNA microarray analysis. Gene Expr. 9:291–304; 2001.
10. Claudel, T.; Leibowitz, M. D.; Fievet, C.; Tailleux, A.; Wagner, B.; Repa, J. J.; Torpier, G.; Lobaccaro, J. M.; Paterniti, J. R.; Mangelsdorf, D. J.; Heyman, R. A.; Auwerx, J. Reduction of atherosclerosis in apolipoprotein E knockout mice by activation of the retinoid X receptor. Proc. Natl. Acad. Sci. USA 98:2610–2615; 2001.
11. Costet, P.; Legendre, C.; More, J.; Edgar, A.; Galtier, P.; Pineau, T. Peroxisome proliferator-activated receptor alpha-isoform deficiency leads to progressive dyslipidemia with sexually dimorphic obesity and steatosis. J. Biol. Chem. 273:29577–29585; 1998.
12. Duvic, M.; Hymes, K.; Heald, P.; Breneman, D.; Martin, A. G.; Myskowski, P.; Crowley, C.; Yocum, R. C. Bexarotene is effective and safe for treatment of refractory advanced-stage cutaneous T-cell lymphoma: Multinational phase II–III trial results. J. Clin. Oncol. 19:2456–2471; 2001.
13. Esteva, F. J.; Glaspy, J.; Baidas, S.; Laufman, L.; Hutchins, L.; Dickler, M.; Tripathy, D.; Cohen, R.; DeMichele, A.; Yocum, R. C.; Osborne, C. K.; Hayes, D. F.; Hortobagyi, G. N.; Winer, E.; Demetri, G. D. Multicenter phase II study of oral bexarotene for patients with metastatic breast cancer. J. Clin. Oncol. 21: 999 1006; 2003.
14. Forman, B. M.; Umesono, K.; Chen, J.; Evans, R. M. Unique response pathways are established by allosteric interactions among nuclear hormone receptors. Cell 81:541–550; 1995.

15. Forman, B. M.; Goode, E.; Chen, J.; Oro, A. E.; Bradley, D. J.; Perlmann, T.; Noonan, D. J.; Burka, L. T.; McMorris, T.; Lamph, W. W.; et al. Identification of a nuclear receptor that is activated by farnesol metabolites. Cell 81:687–693; 1995.
16. Galetto, R.; Albajar, M.; Polanco, J. I.; Zakin, M. M.; Rodriguez-Rey, J. C. Identification of a peroxisome-proliferator-activated-receptor response element in the apolipoprotein E gene control region. Biochem. J. 357: 521–527; 2001.
17. Gampe, R. T., Jr.; Montana, V. G.; Lambert, M. H.; Miller, A. B.; Bledsoe, R. K.; Milburn, M. V.; Kliewer, S. A.; Willson, T. M.; Xu, H. E. Asymmetry in the PPARgamma/RXRalpha crystal structure reveals the molecular basis of heterodimerization among nuclear receptors. Mol. Cell 5:545–555; 2000.
18. Germain, P.; Iyer, J.; Zechel, C.; Gronemeyer, H. Co-regulator recruitment and the mechanism of retinoic acid receptor synergy. Nature 415:187–192; 2002.
19. Itoh, S.; Yoshimura, T.; Iemura, O.; Yamada, E.; Tsujikawa, K.; Kohama, Y.; Mimura, T. Molecular cloning of 25-hydroxyvitamin D-3 24-hydroxylase (Cyp-24) from mouse kidney: Its inducibility by vitamin D-3. Biochim. Biophys. Acta 1264:26–28; 1995.
20. Jackson, J. P.; Ferguson, S. S.; Moore, R.; Negishi, M.; Goldstein, J. A. The constitutive active/androstane receptor regulates phenytoin induction of Cyp2c29. Mol. Pharmacol. 65:1397–1404; 2004.
21. Laffitte, B. A.; Repa, J. J.; Joseph, S. B.; Wilpitz, D. C.; Kast, H. R.; Mangelsdorf, D. J.; Tontonoz, P. LXRs control lipid-inducible expression of the apolipoprotein E gene in macrophages and adipocytes. Proc. Natl. Acad. Sci. USA 98:507–512; 2001.
22. Lampen, A.; Meyer, S.; Nau, H. Effects of receptor-selective retinoids on CYP26 gene expression and metabolism of all-trans-retinoic acid in intestinal cells. Drug Metab. Dispos. 29:742–747; 2001.
23. Lee, S. S.; Pineau, T.; Drago, J.; Lee, E. J.; Owens, J. W.; Kroetz, D. L.; Fernandez-Salguero, P. M.; Westphal, H.; Gonzalez, F. J. Targeted disruption of the alpha isoform of the peroxisome proliferator-activated receptor gene in mice results in abolishment of the pleiotropic effects of peroxisome proliferators. Mol. Cell. Biol. 15:3012–3022; 1995.
24. Lehmann, J. M.; Jong, L.; Fanjul, A.; Cameron, J. F.; Lu, X. P.; Haefner, P.; Dawson, M. I.; Pfahl, M. Retinoids selective for retinoid X receptor response pathways. Science 258:1944–1946; 1992.
25. Li, D.; Li, T.; Wang, F.; Tian, H.; Samuels, H. H. Functional evidence for retinoid X receptor (RXR) as a nonsilent partner in the thyroid hormone receptor/RXR heterodimer. Mol. Cell. Biol. 22:5782–5792; 2002.
26. Loudig, O.; Babichuk, C.; White, J.; Abu-Abed, S.; Mueller, C.; Petkovich, M. Cytochrome P450RAI (CYP26) promoter: A distinct composite retinoic acid response element underlies the complex regulation of retinoic acid metabolism. Mol. Endocrinol. 14:1483–1497; 2000.
27. Luu, L.; Ramshaw, H.; Tahayato, A.; Stuart, A.; Jones, G.; White, J.; Petkovich, M. Regulation of retinoic acid metabolism. Adv. Enzyme Regul. 41:159–175; 2001.
28. Mangelsdorf, D. J.; Evans, R. M. The RXR heterodimers and orphan receptors. Cell 83:841–850; 1995.
29. Marikar, Y.; Wang, Z.; Duell, E. A.; Petkovich, M.; Voorhees, J. J.; Fisher, G. J. Retinoic acid receptors regulate expression of retinoic acid 4-hydroxylase that specifically inactivates all-trans retinoic acid in human keratinocyte HaCaT cells. J. Invest. Dermatol. 111: 434–439; 1998.
30. Minucci, S.; Leid, M.; Toyama, R.; Saint-Jeannet, J. P.; Peterson, V. J.; Horn, V.; Ishmael, J. E.; Bhattacharyya, N.; Dey, A.; Dawid, I. B.; Ozato, K. Retinoid X receptor (RXR) within the RXR-retinoic acid receptor heterodimer binds its ligand and enhances retinoid-dependent gene expression. Mol. Cell. Biol. 17:644–655; 1997.
31. Mistry, M. J.; Clay, M. A.; Kelly, M. E.; Steiner, M. A.; Harmony, J. A. Apolipoprotein E restricts interleukin-dependent T lymphocyte proliferation at the G1A/G1B boundary. Cell. Immunol. 160:14–23; 1995.
32. Mukherjee, R.; Strasser, J.; Jow, L.; Hoener, P.; Paterniti, J. R., Jr.; Heyman, R. A. RXR agonists activate PPARalpha-inducible genes, lower triglycerides, and raise HDL levels in vivo. Arterioscler. Thromb. Vasc. Biol. 18:272–276; 1998.
33. Mukherjee, R.; Davies, P. J.; Crombie, D. L.; Bischoff, E. D.; Cesario, R. M.; Jow, L.; Hamann, L. G.; Boehm, M. F.; Mondon, C. E.; Nadzan, A. M.; Paterniti, J. R., Jr.; Heyman, R. A. Sensitization of diabetic and obese mice to insulin by retinoid X receptor agonists. Nature 386:407–410; 1997.
34. Niederreither, K.; Vermot, J.; Fraulob, V.; Chambon, P.; Dolle, P. Retinaldehyde dehydrogenase 2 (RALDH2)-independent patterns of retinoic acid synthesis in the mouse embryo. Proc. Natl. Acad. Sci. USA 99:16111–16116; 2002.
35. Ouamrane, L.; Larrieu, G.; Gauthier, B.; Pineau, T. RXR activators molecular signalling: Involvement of a PPAR alpha-dependent pathway in the liver and kidney, evidence for an alternative pathway in the heart. Br. J. Pharmacol. 138:845–854; 2003.
36. Pascussi, J. M.; Robert, A.; Nguyen, M.; Walrant-Debray, O.; Garabedian, M.; Martin, P.; Pineau, T.; Saric, J.; Navarro, F.; Maurel, P.; Villarem, M. J. Drug-activated pregnane X receptor enhances CYP24 expression: Possible involvement in drug-induced osteomalacia. J. Clin. Invest. 115:177–186; 2005.
37. Perlmann, T.; Jansson, L. A novel pathway for vitamin A signaling mediated by RXR heterodimerization with NGFI-B and NURR1. Genes Dev. 9:769–782; 1995.
38. Reue, K. L.; Quon, D. H.; O'Donnell, K. A.; Dizikes, G. J.; Fareed, G. C.; Lusis, A. J. Cloning and regulation of messenger RNA for mouse apolipoprotein E. J. Biol. Chem. 259:2100–2107; 1984.
39. Rizvi, N. A.; Marshall, J. L.; Dahut, W.; Ness, E.; Truglia, J. A.; Loewen, G.; Gill, G. M.; Ulm, E. H.; Geiser, R.; Jaunakais, D.; Hawkins, M. J. A Phase I study of LGD1069 in adults with advanced cancer. Clin. Cancer Res. 5:1658–1664; 1999.

40. Takeyama, K.; Kitanaka, S.; Sato, T.; Kobori, M.; Yanagisawa, J.; Kato, S. 25-Hydroxyvitamin D3 1alpha-hydroxylase and vitamin D synthesis. Science 277: 1827–1830; 1997.
41. Tzameli, I.; Chua, S. S.; Cheskis, B.; Moore, D. D. Complex effects of rexinoids on ligand dependent activation or inhibition of the xenobiotic receptor, CAR. Nucl. Recept. 1:2; 2003.
42. Vogel, T.; Guo, N. H.; Guy, R.; Drezlich, N.; Krutzsch, H. C.; Blake, D. A.; Panet, A.; Roberts, D. D. Apolipoprotein E: a potent inhibitor of endothelial and tumor cell proliferation. J. Cell. Biochem. 54:299–308; 1994.
43 Willy, P. J.; Umesono, K.; Ong, E. S.; Evans, R. M.; Heyman, R. A.; Mangelsdorf, D. J. LXR, a nuclear receptor that defines a distinct retinoid response pathway. Genes Dev. 9:1033–1045; 1995.
44. Xie, W.; Barwick, J. L.; Simon, C. M.; Pierce, A. M.; Safe, S.; Blumberg, B.; Guzelian, P. S.; Evans, R. M. Reciprocal activation of xenobiotic response genes by nuclear receptors SXR/PXR and CAR. Genes Dev. 14: 3014–3023; 2000.
45. Yamamoto, Y.; Zolfaghari, R.; Ross, A. C. Regulation of CYP26 (cytochrome P450RAI) mRNA expression and retinoic acid metabolism by retinoids and dietary vitamin A in liver of mice and rats. FASEB J. 14: 2119–2127; 2000.
46. Yamazaki, K.; Kuromitsu, J.; Tanaka, I. Microarray analysis of gene expression changes in mouse liver induced by peroxisome proliferator-activated receptor alpha agonists. Biochem. Biophys. Res. Commun. 290: 1114–1122; 2002.
47. Zou, A.; Elgort, M. G.; Allegretto, E. A. Retinoid X receptor (RXR) ligands activate the human 25-hydroxyvitamin D3-24-hydroxylase promoter via RXR heterodimer binding to two vitamin D-responsive elements and elicit additive effects with 1,25-dihydroxyvitamin D3. J. Biol. Chem. 272:19027–19034; 1997.